Analytic I-Love-C relations for realistic neutron stars

Nan Jiang◯ and Kent Yagi◯

Department of Physics, University of Virginia, Charlottesville, Virginia 22904, USA

Recent observations of neutron stars with radio, x rays, and gravitational waves have begun to constrain the equation of state for nuclear matter beyond the nuclear saturation density. To one's surprise, there exist approximate universal relations connecting certain bulk properties of neutron stars that are insensitive to the underlying equation of state and having important applications on probing fundamental physics including nuclear and gravitational physics. To date, analytic works on universal relations for *realistic* neutron stars are lacking, which may lead to a better understanding of the origin of the universality. Here, we focus on the universal relations between the compactness ($\mathcal{C}$), the moment of inertia (I), and the tidal deformability (related to the Love number) and derive analytic, approximate I-Love-C relations. To achieve this, we construct slowly rotating and tidally deformed neutron star solutions analytically starting from an extended Tolman VII model that accurately describes nonrotating realistic neutron stars, which allows us to extract the moment of inertia and the tidal deformability on top of the compactness. We solve the field equations analytically by expanding them about the Newtonian limit and keeping up to sixth order in the stellar compactness. Based on these analytic solutions, we can mathematically demonstrate the $\mathcal{O}(10\%)$ equation-of-state variation in the I-C and Love-C relations and the $\mathcal{O}(1\%)$ variation in the I-Love relation that have previously been found numerically. Our new analytic relations agree more accurately with numerical results for realistic neutron stars (especially the I-C and Love-C ones) than the analytic relations for constant-density stars derived in previous work. Based on these analytic findings, we attribute a possible origin of the universality for the I-C and Love-C relations to the fact that the energy density of realistic neutron stars can be approximated as a quadratic function, as is the case for the Tolman VII solution.

I. INTRODUCTION

Neutron stars (NSs) are unique astrophysical objects for studying fundamental physics, in particular, strongly interacting many-body systems in nuclear physics [1]. The energy density can reach up to several times the nuclear saturation density in their inner cores, which are difficult to access with terrestrial nuclear experiments.

The relation between the mass and radius of a NS depends strongly on the equation of state (EOS) of nuclear matter, the relation between energy density and pressure. This, in turn, means that one can probe the EOS by measuring the NS mass and radius independently [2–7]. For example, the x-ray payload NICER at the International Space Station recently measured the mass and radius of a pulsar to ~10% accuracy [8–13], which has been used to constrain the EOS and measure nuclear matter parameters [13–18]. Mass measurements of heavy NSs also help to constrain the EOS [19–21].

There are several other important global observables of NSs besides mass and radius that are useful for probing nuclear physics. Moment of inertia I is expected to be measured from future observations of the double-pulsar system [22]. A useful constraint on the EOS can be made if I can be determined up to about 10% [23]. Tidal deformability (related to the tidal Love number), that is a linear response of an object's quadrupole moment to the external tidal field, is encoded in gravitational waves (GWs) from binary NS mergers [24,25]. The recent GW event GW170817 provides a first measurement of the tidal deformability [26], which has been used to constrain the EOS and nuclear matter parameters [27–39].

Unlike the mass-radius relation, which depends strongly on the underlying EOS, there exist universal relations among certain NS observables that do not depend sensitively on the stellar internal structure (see, e.g., [40,41] for recent reviews). One example is among the moment of inertia I, the tidal Love number (or the tidal deformability), and the quadrupole moment Q, which are commonly known as the I-Love-Q relations [42,43]. The relations are universal with an EOS variation of ~1%. Similar relations were discovered among tidal parameters in gravitational waveforms from binary NSs, known as the binary Love relations [44,45]. These relations can be used to break degeneracies among parameters in GW signals, enhancing the measurability of the tidal effects directly related to the EOS [26]. The relations have many other interesting applications, including astrophysics, gravitational physics, and cosmology [42–45]. Reference [46] proposed emergent, approximate symmetry

related to isodensity contours inside NSs as a possible origin of the universality. Reference [47] proposed that the universality is due to the realistic EOSs being "close" to the incompressible, constant-density one, which agrees with the picture of Ref. [46], since the approximate symmetry becomes exact in the incompressible limit.

Most of the works on NS universal relations focused on numerical calculations, though there are a limited number of works within an analytic framework. The amount of universality in the I-Love relation was analytically explained in the Newtonian limit by comparing the $n = 0$ and $n = 1$ polytropes [42,43]. Reference [48] derived the analytic, I-Love relation for constant-density stars that is applicable to both the Newtonian and relativistic regimes. The authors studied the relation between the moment of inertia and compactness (the I-C relation) and that between the tidal deformability and compactness (the Love-C relation) in terms of a series expansion in compactness. The authors then eliminated the compactness to find the analytic I-Love relation. Since constant-density stars are more appropriate for describing quark stars, what is still missing is the analytic, I-Love-C relations for *realistic* NSs and to study analytically the amount of the EOS variation in these relations.

One useful, analytic model of nonrotating realistic NSs is the Tolman VII solution [1,49]. This is a two-parameter (mass and radius) solution to the Einstein equations, in which the energy-density profile inside a star is approximated by a quadratic function in a radial coordinate. In Ref. [50], we improved this model further by extending the energy-density profile to a quartic function. We introduced a phenomenological parameter α to more accurately capture the realistic energy-density profiles. We found that this modified Tolman VII model has an improved accuracy for describing the metric and pressure or energy-density functions over the original Tolman VII solution by a factor of 2–5.

In this paper, we construct analytic, I-Love-C relations for realistic NSs by extending nonrotating solutions for the modified Tolman VII model to slowly rotating or tidally deformed configurations, which allows us to extract the moment of inertia and tidal deformability. We treat the rotation or tidal deformation to be a small perturbation and keep only to leading order in such a perturbation. This is a good approximation since, e.g., the rotation of the primary pulsar in the double-pulsar binary is much smaller than the breakup rotation. Following Ref. [48], we find a series-expanded solution for the moment of inertia and the tidal deformability in terms of compactness. We then eliminate the compactness to find the I-Love relation for the modified Tolman VII model applicable to realistic NSs. Varying the phenomenological parameter α within a reasonable range for realistic NSs allows us to analytically estimate the amount of the universality in the I-Love-C relations.

A. Executive summary

We first constructed analytic I-C and Love-C relations for the original Tolman VII solution in terms of a series expansion in compactness. After resumming the series via the Padé method as done in Ref. [47] for constant-density stars, we arrived at

$$\bar{I}_{\text{Tol}} = \frac{\sum_{j=0}^{3} c_j^{(\bar{I})} \mathcal{C}^j}{2\mathcal{C}^3 \sum_{i=0}^{3} d_i^{(\bar{I})} \mathcal{C}^i}, \tag{1}$$

$$\begin{aligned} \bar{\lambda} = &\frac{16}{15} (1 - 2\mathcal{C})^2 [2 + 2\mathcal{C}(y_R - 1) - y_R]/ \\ &\{2\mathcal{C}[6 - 3y_R + 3\mathcal{C}(5y_R - 8)] \\ &+ 4\mathcal{C}^3 [13 - 11y_R + \mathcal{C}(3y_R - 2) + 2\mathcal{C}^2(1 + y_R)] \\ &+ 3(1 - 2\mathcal{C})^2 [2 - y_R + 2\mathcal{C}(y_R - 1)] \ln(1 - 2\mathcal{C})\}, \end{aligned} \tag{2}$$

with

$$y_{R,\text{Tol}} = \frac{\sum_{j=0}^{2} c_j^{(\bar{\lambda})} \mathcal{C}^j}{\sum_{i=0}^{2} d_i^{(\bar{\lambda})} \mathcal{C}^i}, \tag{3}$$

where the coefficients c_i and d_i are given in Table I. We also present these analytic relations in a supplemental *Mathematica* notebook [51]. Here the subscript "Tol" stands for the original Tolman VII solution.

Figure 1 compares these analytic relations with numerical ones for NSs with realistic EOSs and the analytic one for constant-density stars. Observe that the analytic relations for the Tolman VII model can accurately describe the

TABLE I. Coefficients $c_i^{(\bar{I})}$ and $d_i^{(\bar{I})}$ in Eq. (1) and $c_i^{(\bar{\lambda})}$ and $d_i^{(\bar{\lambda})}$ in Eq. (3).

| Coefficient	Value
$c_0^{(\bar{I})}$	0
$c_1^{(\bar{I})}$	$\frac{4}{7}$
$c_2^{(\bar{I})}$	$-\frac{4475212734657724923440}{3819744665891770040271}$
$c_3^{(\bar{I})}$	$\frac{5251205464431025417380426}{1199208837856721204143080445}$
$d_0^{(\bar{I})}$	1
$d_1^{(\bar{I})}$	$-\frac{52610171361202024028}{16535691194336666841}$
$d_2^{(\bar{I})}$	$\frac{73157107800621748853 66}{2662246282288203361401}$
$d_3^{(\bar{I})}$	$-\frac{246827646012322907030 83888}{472948052048499327152887 65}$
$c_0^{(\bar{\lambda})}$	$\frac{75974923394}{756262478125}$
$c_1^{(\bar{\lambda})}$	$\frac{3752041566032080345751403133284738094796 2712}{411377240187178971792302428103500257711562 5}$
$c_2^{(\bar{\lambda})}$	$\frac{95969210152550100139259108607856780700459239 7}{921485018019280896814757438951840577273900 0}$
$d_0^{(\bar{\lambda})}$	1
$d_1^{(\bar{\lambda})}$	$\frac{125977972708997462470931885904739}{16737259354597288810791427662 12}$
$d_2^{(\bar{\lambda})}$	$-\frac{11560237280939583134679473198513569}{70296489289308613005323996180904}$
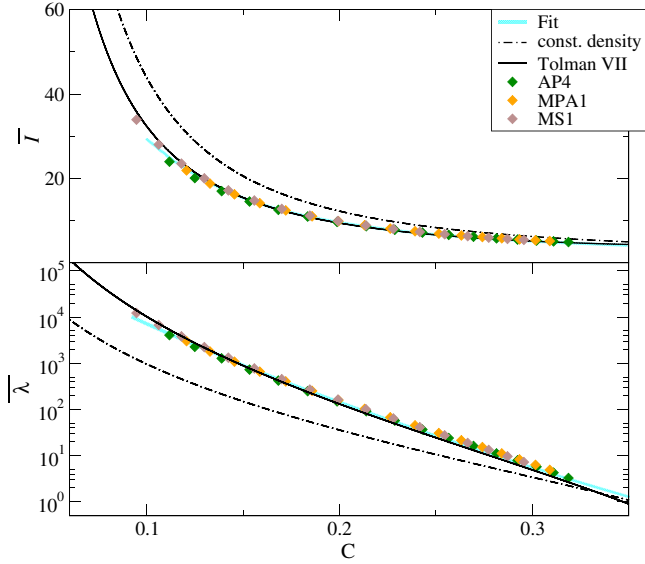
FIG. 1. Approximate, analytic I-C relation (top) and Love-C relation (bottom) for the original Tolman VII model (solid curve) for realistic NSs and constant-density-star model [48] (dot-dashed curve), both in Padé resummed form. We also present those for realistic EOSs representing soft (AP4), intermediate (MPA1), and stiff (MS1) EOS classes. We can see a clear improvement in accuracy for the Tolman-VII curves over the constant-density ones in both panels. For comparison, the numerical fit curves in Ref. [40] are plotted in cyan.

realistic relations. We can see that the analytic curves are very close to the numerical fit ones in Ref. [40], with fractional differences ∼1% for the I-C curve and several percent for the Love-C curve. Observe also that the former is much more accurate than the one for constant-density stars, which is more appropriate for quark stars. We next constructed the I-Love relation semianalytically for the original Tolman VII solution by eliminating the compactness from the I-C and Love-C relations, which again accurately models the numerical results.

We also derived the analytic I-C and Love-C and semi-analytic I-Love relations for the modified Tolman VII model [50]. By varying the density profile parameter α that corresponds to varying the EOS, we successfully obtained the 10% EOS variation in the I-C and Love-C relations while 1% EOS variation in the I-Love relations, which agree with previous numerical findings [40,42,43,52,53].

1. Organization

The organization of the rest of the paper is as follows. In Sec. II, we briefly introduce what original and modified Tolman VII solutions are. In Secs. III and IV, we describe how we construct the analytic I-C and Love-C relations, respectively, and compare them against numerical relations for realistic NSs and analytic relations for constant-density stars. We also analytically estimate the amount of universality in these relations. In Sec. V, we present the results of

the semianalytic I-Love relation. In Sec. VI, we use our analytic findings to present a possible origin of the universality for the I-C and Love-C relations. In Sec. VII, we conclude and give possible directions for future work. We use the geometric units of $c = 1$ and $G = 1$ throughout this paper.

II. MODIFIED TOLMAN VII SOLUTION

Here, we briefly review the original Tolman VII [49] and modified Tolman VII [50] solution of a static, isolated, and spherically symmetric NS in the interior region. We use the metric ansatz given by

$$ds^2 = ds_0^2 \equiv -e^\nu dt^2 + e^\lambda dr^2 + r^2(d\theta^2 + \sin^2\theta d\phi^2), \quad (4)$$

where ν and λ are functions of r. We also assume that matter inside a NS is modeled by a perfect fluid with the stress-energy tensor given by

$$T_{\mu\nu} = (\rho + p)u_\mu u_\nu + pg_{\mu\nu}. \quad (5)$$

Here ρ represents energy density, p represents pressure, and u_μ is the 4-velocity of the fluid. Substituting Eqs. (4) and (5) into the Einstein equations, one finds the following three differential equations with four unknown quantities (ν, λ, p, and ρ, which are functions of r only) [49]:

$$\frac{d}{dr}\left(\frac{e^{-\lambda} - 1}{r^2}\right) + \frac{d}{dr}\left(\frac{e^{-\lambda}\nu'}{2r}\right) + e^{-\lambda-\nu}\frac{d}{dr}\left(\frac{e^\nu\nu'}{2r}\right) = 0, \quad (6)$$

$$e^{-\lambda}\left(\frac{\nu'}{r} + \frac{1}{r^2}\right) - \frac{1}{r^2} = 8\pi p, \quad (7)$$

$$\frac{dm}{dr} = 4\pi r^2 \rho, \quad (8)$$

where a prime denotes a derivative with respect to r and

$$e^{-\lambda} \equiv 1 - \frac{2m(r)}{r} \quad (9)$$

with $m(r)$ representing the mass enclosed in a sphere of radius r.

To make the system of equations closed, one typically specifies an EOS relating p as a function of ρ. Instead, in this paper, we specify the radial profile of ρ, which corresponds to choosing an EOS.

In the exterior region ($r > R$), $p_{\text{ext}} = 0$, $\rho_{\text{ext}} = 0$, and $m(r) = M$ with the stellar mass M. Then, we have

$$e^{\nu_{\text{ext}}} = e^{-\lambda_{\text{ext}}} = 1 - \frac{2M}{r}. \quad (10)$$

A. Original Tolman VII solution

In the original Tolman VII solution [49], the energy-density profile is given by

$$\rho_{\text{Tol}}(\xi) = \rho_c(1 - \xi^2). \tag{11}$$

Here the dimensionless radial coordinate ξ is given by $\xi = r/R$ with the stellar radius R and ρ_c is the central energy density. The subscript "Tol" indicates the quantity for the original Tolman VII solution. We next substitute the above density profile into Eq. (8) and integrate over r under the boundary condition $m(0) = 0$. One finds

$$m_{\text{Tol}}(r) = 4\pi\rho_c \left(\frac{r^3}{3} - \frac{r^5}{5R^2}\right). \tag{12}$$

ρ_c can be expressed in terms of R and the stellar compactness $\mathcal{C} \equiv M/R$ as

$$\rho_c = \frac{15\mathcal{C}}{8\pi R^2}. \tag{13}$$

We can substitute this into Eqs. (11) and (12) to find

$$\rho_{\text{Tol}}(\xi) = \frac{15\mathcal{C}}{8\pi R^2}(1 - \xi^2), \tag{14}$$

$$m_{\text{Tol}}(\xi) = \mathcal{C}R \left(\frac{5}{2}\xi^3 - \frac{3}{2}\xi^5\right). \tag{15}$$

Using Eq. (9), $e^{-\lambda}$ is given by

$$e^{-\lambda_{\text{Tol}}(\xi)} = 1 - \mathcal{C}\xi^2(5 - 3\xi^2). \tag{16}$$

Next, one can solve for ν and p to find

$$e^{\nu_{\text{Tol}}(\xi)} = C_1^{\text{Tol}}\cos^2\phi_{\text{Tol}}, \tag{17}$$

$$p_{\text{Tol}}(\xi) = \frac{1}{4\pi R^2}\left[\sqrt{3\mathcal{C}e^{-\lambda_{\text{Tol}}}}\tan\phi_{\text{Tol}} - \frac{\mathcal{C}}{2}(5 - 3\xi^2)\right], \tag{18}$$

respectively, with

$$\phi_{\text{Tol}}(\xi) = C_2^{\text{Tol}} - \frac{1}{2}\log\left(\xi^2 - \frac{5}{6} + \sqrt{\frac{e^{-\lambda_{\text{Tol}}}}{3\mathcal{C}}}\right), \tag{19}$$

and the integration constants are given by

$$C_1^{\text{Tol}} = 1 - \frac{5\mathcal{C}}{3}, \tag{20}$$

$$C_2^{\text{Tol}} = \arctan\sqrt{\frac{\mathcal{C}}{3(1 - 2\mathcal{C})}} + \frac{1}{2}\log\left(\frac{1}{6} + \sqrt{\frac{1 - 2\mathcal{C}}{3\mathcal{C}}}\right). \tag{21}$$
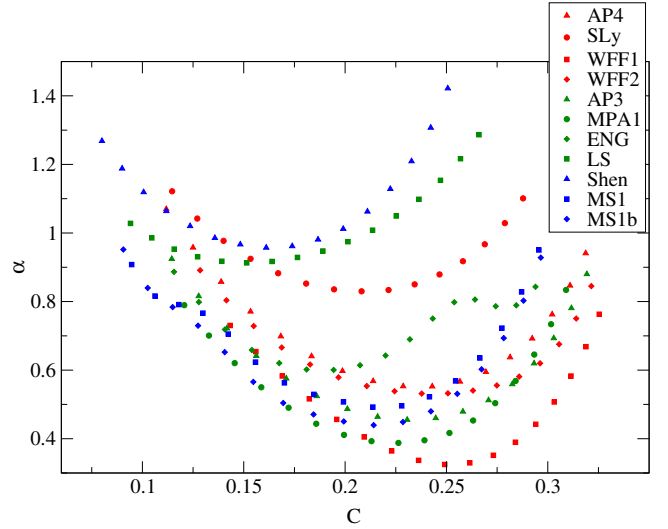
The above solution is the so-called Tolman VII solution.

FIG. 2. The parameter α introduced in the density profile of the modified Tolman VII model [Eq. (22)] against the compactness $\mathcal{C}$ for 11 realistic EOSs. The red, green, and blue dots represent soft, intermediate, and stiff EOSs, respectively.

B. Modified Tolman VII solution

The modified Tolman VII model [50] introduces an additional term to Eq. (11) with a free parameter α in order to capture the variation in the energy-density profile among different EOSs:

$$\rho_{\text{mod}}(\xi) = \rho_c[1 - \alpha\xi^2 + (\alpha - 1)\xi^4]. \tag{22}$$

Obviously, this new profile reduces to the original one in the limit $\alpha \to 1$. Figure 2 presents α obtained by fitting a numerical energy-density profile with Eq. (22) for various EOSs[1] and compactness. Observe that α ranges in $\alpha \in [0.4, 1.4]$ when $\mathcal{C} \in [0.05, 0.35]$. We will vary α within this range in later calculations.

The remaining equations are modified from the original Tolman VII one as follows. m and λ now become

$$m_{\text{mod}}(\xi) = 4\pi\rho_c R^3\xi^3\left(\frac{1}{3} - \frac{\alpha}{5}\xi^2 + \frac{\alpha - 1}{7}\xi^4\right), \tag{23}$$

$$e^{-\lambda_{\text{mod}}(\xi)} = 1 - 8\pi R^2\xi^2\rho_c\left(\frac{1}{3} - \frac{\alpha}{5}\xi^2 + \frac{\alpha - 1}{7}\xi^4\right), \tag{24}$$

respectively, with the subscript "mod" representing the quantities in the modified Tolman solution. The expressions for ν and p are then adjusted to be

$$e^{\nu_{\text{mod}}(\xi)} = C_1^{\text{mod}}\cos^2\phi_{\text{mod}}, \tag{25}$$

---

[1]The 11 EOSs considered here are same as those in Ref. [50], which all support NSs with their mass above $2 M_\odot$.

$$p_{\text{mod}}(\xi) = \sqrt{\frac{e^{-\lambda_{\text{Tol}}}\rho_c}{10\pi}\frac{\tan\phi_{\text{mod}}}{R} + \frac{1}{15}(3\xi^2 - 5)\rho_c}$$
$$+ \frac{6(1-\alpha)\rho_c}{16\pi(10-3\alpha)\rho_c R^2 - 105}, \qquad (26)$$

respectively, with

$$\phi_{\text{mod}}(\xi) = C_2^{\text{mod}} - \frac{1}{2}\log\left(\xi^2 - \frac{5}{6} + \sqrt{\frac{5e^{-\lambda_{\text{Tol}}}}{8\pi R^2\rho_c}}\right), \quad (27)$$

$$C_1^{\text{mod}} = (1 - 2C)\left\{1 + \frac{8\pi R^2\rho_c(10-3\alpha)^2(15-16\pi R^2\rho_c)}{3[105 + 16\pi R^2\rho_c(3\alpha-10)]^2}\right\}, \qquad (28)$$

$$C_2^{\text{mod}} = \arctan\left[-\frac{2(10-3\alpha)R\sqrt{6\pi\rho_c(15-16\pi\rho_c R^2)}}{48\pi(10-3\alpha)\rho_c R^2 - 315}\right]$$
$$+ \frac{1}{2}\log\left(\frac{1}{6} + \sqrt{\frac{5}{8\pi\rho_c R^2} - \frac{2}{3}}\right). \qquad (29)$$

Notice that the above solution is parameterized by $(C, R, \rho_c,$ and $\alpha)$. We can further eliminate ρ_c from the condition $M = m_{\text{mod}}(1)$, which yields

$$\rho_c = \frac{105C}{8\pi R^2(10-3\alpha)}. \qquad (30)$$

Using this in the modified Tolman VII expressions, we obtain a three-parameter (C, R, α) [or, equivalently, (M, R, α)] model which will be used in the following calculations.

III. MOMENT OF INERTIA

A. Formulation

One can extract the moment of inertia I from the asymptotic behavior of the time-spatial component of the metric at infinity for a slowly rotating NS. For simplicity, we consider uniform rotation. The metric ansatz is given by

$$ds^2 = ds_0^2 - 2\Omega(1-\omega)r^2\sin^2\theta dtd\phi, \qquad (31)$$

where ds_0^2 is the nonrotating part of the line element in Eq. (4), Ω is the constant stellar angular velocity, and ω is a function of r (or ξ). Substituting this ansatz into the Einstein equations, one finds an equation for ω as [54]

$$\frac{d}{d\xi}\left(\xi^4 j\frac{d\omega}{d\xi}\right) + 4\xi^3\frac{dj}{d\xi}\omega = 0, \qquad (32)$$

with the boundary condition

$$\omega|_{\xi\to 0} = 1, \qquad \frac{d\omega}{d\xi}\bigg|_{\xi\to 0} = 0, \qquad (33)$$

and $j(\xi) = e^{(-\lambda+\nu)/2}$.

Let us next look at the exterior solution. Integrating the equation in the exterior region [with $j(\xi) = 1$], one finds

$$\omega_{\text{ext}}(r) = 1 - \frac{2I}{r^3}. \qquad (34)$$

The closed form of I can be obtained easily from the differential equations and its boundary conditions above, which is [54]

$$I = \frac{8\pi R^5}{3}\int_0^1 \frac{\xi^5(p+\rho)e^{-(\nu+\lambda)/2}\omega}{\xi - \frac{2m}{R}}d\xi. \qquad (35)$$

B. Analytic solutions

We now find an analytic solution to Eq. (32) for the modified Tolman VII solution. Unfortunately, we were not able to find an exact solution. Instead, we apply a post-Minkowskian recursive perturbation method adopted by Chan, Chan, and Leung [48] for incompressible stars to derive an approximate, analytic solution for ω and I.

We begin by defining

$$\tilde{\omega}(\xi) \equiv 1 - \omega(\xi) \qquad (36)$$

and expanding $\tilde{\omega}(\xi)$ and $j(\xi)$ in power series of C:

$$\tilde{\omega}(\xi, C) \approx \sum_{n=0}^{N}\tilde{\omega}_n(\xi)C^n, \qquad j(\xi, C) \approx \sum_{n=0}^{N}j_n(\xi)C^n. \qquad (37)$$

Here $\tilde{\omega}_n(\xi)$ and $j_n(\xi)$ are functions of ξ only, while N corresponds to the order of the expansion that we keep. In the Newtonian limit $(C \to 0)$, one finds

$$j_0(\xi) = 1, \qquad \tilde{\omega}_0(\xi) = 0. \qquad (38)$$

Having the above series expansion at hand, we can solve the differential equation. Namely, we substitute Eq. (37) into Eq. (32) and solve the latter for $\tilde{\omega}_n$ order by order in powers of C. We can then derive the series expansion of the dimensionless moment of inertia from Eq. (35) as

$$\bar{I} \equiv \frac{I}{M^3} \approx \sum_{n=0}^{N}\bar{I}_n C^{n-2}. \qquad (39)$$

The series starts with C^{-2}, since $I \propto MR^2$ in the Newtonian limit. $\bar{I}$ is given in terms of $\tilde{\omega}$ as

$$\bar{I} = \frac{\tilde{\omega}_R}{2C^3}, \qquad \tilde{\omega}_R \equiv \tilde{\omega}(\xi = 1). \qquad (40)$$

Figure 3 shows how the I-C series converges as one increases the order of expansion. Observe that the
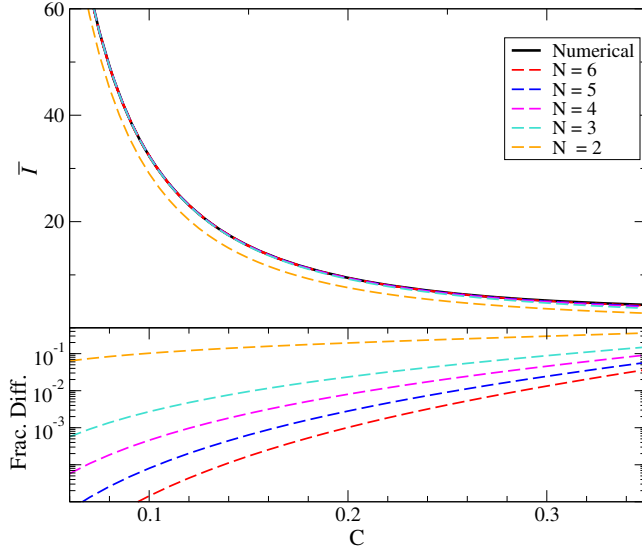
FIG. 3. (Top) I-C relation for the original Tolman VII solution with different orders of series expansion in $\mathcal{C}$. (Bottom) Fractional differences between the curve obtained numerically and the analytic one at each expansion order. Observe that the analytic relation converges as we increase the order.
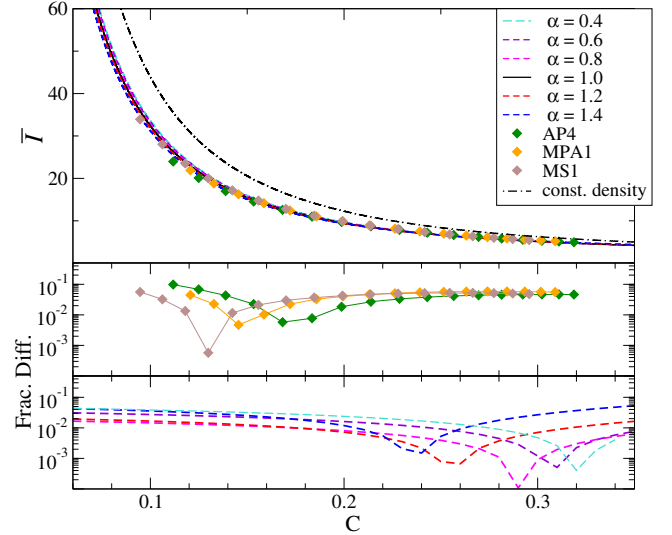

FIG. 4. (Top) Approximate, analytic I-C relation (up to sixth order in the series expansion in $\mathcal{C}$) for the modified Tolman VII solution with five representative values of α. For comparison, we also show the numerical relation for three representative realistic EOSs, namely, AP4 (soft), MPA1 (intermediate), and MS1 (stiff). The dot-dashed line represents the relation for incompressible constant-density stars in Ref. [48]. (Middle) Relative fractional difference of the I-C relation for the realistic EOSs from that for the original Tolman solution. (Bottom) Relative fractional difference for the modified Tolman VII relation from the original one. Observe that the EOS variation is kept under 10% for both realistic EOSs and modified Tolman VII relations, in agreement with that for realistic EOSs in Fig. 15 of Ref. [40].

expansion to sixth order in compactness can accurately describe the numerical relation. Since the expressions for $\bar{I}_n$ are lengthy and not illuminating, we show them in a supplemental *Mathematica* notebook [51].

We present in the top panel in Fig. 4 the approximate, analytic I-C relation for the modified Tolman VII solution. For comparison, we also show the approximate, analytic relation for incompressible stars [48] and the relations for some representative realistic EOSs. Observe that the new analytic relation can beautifully approximate the numerical relation for the realistic EOSs. Observe also that the relation for incompressible stars found in Ref. [48] does not provide an accurate description for realistic NSs.[2] The new relation found in this paper gives us the first analytic expression for the I-C relation for realistic NSs other than the fits in, e.g., Refs. [40,55,56].

The bottom panel shows the fractional difference of the modified Tolman VII relation from the original one. Notice that, when we vary α within the range for realistic EOSs, the analytic relation varies by $\sim$10%. This amount agrees with that of the EOS variation in the relation for realistic NSs in the middle panel (see also [40]). Thus, the new relation provides us an analytic explanation for the amount of universality in the I-C relation.

Let us investigate further the EOS variation in the I-C relation using the new analytic I-C relation. Expanding $\bar{I}_n$ about $\alpha = 1$ (the original Tolman solution), we find

$$\bar{I}_0 = 0.286[1 - 0.105(\alpha - 1) + \mathcal{O}(\alpha - 1)^2],$$
$$\bar{I}_1 = 0.323[1 - 0.100(\alpha - 1) + \mathcal{O}(\alpha - 1)^2],$$
$$\bar{I}_2 = 0.462[1 + 0.258(\alpha - 1) + \mathcal{O}(\alpha - 1)^2],$$
$$\bar{I}_3 = 0.732[1 + 0.403(\alpha - 1) + \mathcal{O}(\alpha - 1)^2],$$
$$\bar{I}_4 = 1.226[1 + 0.545(\alpha - 1) + \mathcal{O}(\alpha - 1)^2],$$
$$\bar{I}_5 = 2.132[1 + 0.688(\alpha - 1) + \mathcal{O}(\alpha - 1)^2].$$

This shows that the α dependence on the leading contribution to $\bar{I}$ ($\bar{I}_0$) is $\sim$10% (because the relative coefficient is 0.105), and similar for $\bar{I}_1$. This analytically explains the origin of the $\mathcal{O}(10\%)$ EOS variation in the relation. On the other hand, the α dependence becomes larger as we increase n in $\bar{I}_n$, though such contributions are higher order and do not affect the relation much.

IV. TIDAL LOVE NUMBER

A. Formulation

In this section, we present the calculation of the tidal deformability or the tidal Love number due to tidal deformation. For example, a primary NS in a binary acquires tidal deformation due to the tidal field created

---

[2]The relation for incompressible stars can accurately describe the relation for quark stars [40].

by a companion star. Such an effect is characterized by the dimensionless tidal deformability, which is defined as

$$\bar{\lambda} \equiv \frac{\lambda}{M^5} \equiv -\frac{Q}{M^5}\mathcal{E} = \frac{2}{3}k_2\mathcal{C}^{-5}. \qquad (41)$$

Here Q and $\mathcal{E}$ are the tidally induced quadruple moment and the external tidal field, respectively, and k_2 is the tidal Love number defined by $k_2 \equiv (3/2)(\lambda/R^5)$. To calculate Q and $\mathcal{E}$, we follow the formulations and conventions established in Ref. [24]. We begin by the metric ansatz

$$ds^2 = ds_0^2 - [h_2(e^\nu dt^2 + e^\lambda dr^2) \\ - r^2 K_2(d\theta^2 + \sin^2\theta d\phi^2)]Y_{2m}(\theta, \phi), \qquad (42)$$

where $h_2(r)$ and $K_2(r)$ are quadrupolar tidal perturbations while $Y_{\ell m}$ are spherical harmonics. Substituting this into the Einstein equations, one can derive a second-order differential equation for h_2 as [24]

$$\xi y' + y^2 + ye^\lambda[1 + 4\pi\xi^2 R^2(p-\rho)] \\ - \left\{\frac{6e^\lambda}{\xi^2} - 4\pi e^\lambda R^2\left[5\rho + 9p + (\rho+p)\frac{d\rho}{dp}\right] + \nu'^2\right\}\xi^2 = 0, \qquad (43)$$

where

$$y \equiv \frac{\xi}{h_2}\frac{dh_2}{d\xi} \qquad (44)$$

and the prime represents a derivative with respect to ξ. The initial condition is given by $y(\xi = 0) = 2$. Solving the above equation, one can find $\bar{\lambda}$ using Eq. (41) as in Eq. (2) with $y_R \equiv y(\xi = 1)$ [24,57].

B. Analytic solution

We now study analytic expressions for h_2 (or y) and the tidal deformability. Similar to the case of the moment of inertia, we were not able to solve Eq. (43) exactly for the modified Tolman VII model. Thus, we follow the same procedure as before and consider series expansion in $\mathcal{C}$.

We begin by expanding y as [48]

$$y(\xi, \mathcal{C}) \approx \sum_{n=0}^{N} y_n(\xi)\mathcal{C}^n, \qquad (45)$$

where each coefficient y_n is a function of ξ only. Substituting this expansion into Eq. (43) and looking order by order, one can derive differential equations for y_n. Unlike the case of the moment of inertia, we were not able to find analytic exact solutions to these equations for the modified Tolman VII model.[3] Thus, we further expand y_n about $\xi = 0$ as

---

[3]For the original Tolman model, y_0 can be solved exactly in terms of hypergeometric functions, though the differential equation is too complicated to be solved for y_1 and higher.

$$y_n(\xi) \approx \sum_{k=1}^{K} y_n^{(2k)}\xi^{2k}, \qquad (46)$$

where $y_n^{(2k)}$ is now a constant while K is the expansion order in terms of ξ. We expand Eq. (43) in powers of both $\mathcal{C}$ and ξ, find algebraic equations for $y_n^{(2k)}$ order by order, and solve them. We show $y_n(\xi)$ expanded up to 12th order in ξ ($K = 6$) in the supplemental *Mathematica* notebook [51].

Figure 5 compares the analytic relations between $\bar{\lambda}$ and $\mathcal{C}$ (the Love-C relations) for the original Tolman solution at different expansion order in $\mathcal{C}$ against the numerical relation. For the former, we fixed $K = 6$ for the ξ expansion. Unlike the I-C case in Fig. 3, the series does not converge. We found that the sound speed squared $(dp/d\rho)$ in Eq. (43) becomes inaccurate as one goes to higher order in $\mathcal{C}$. The analytic relation is given in series expansion in $\mathcal{C}$; thus, the approximation becomes worse in a large $\mathcal{C}$ region. In this section, we keep up to third order in $\mathcal{C}$ [$N = 3$ in Eq. (45)] and 12th order in ξ [$K = 6$ in Eq. (46)] that most accurately approximates the correct numerical relation. When deriving the I-Love relation, we will use the relation up to sixth order in $\mathcal{C}$ as we will explain in more detail in Sec. V.

The top panel in Fig. 6 presents the analytic Love-C relations for the modified Tolman solution, together with those for the realistic EOSs and the one found in Ref. [48] for constant-density stars. Observe that, similar to Fig. 4, the analytic relation for the modified Tolman solution can accurately describe the results for the realistic EOSs, while that for constant-density stars fails to do so. The bottom panel shows the fractional difference in the Love-C relations between the modified and original Tolman solutions. Observe that the amount of the variation in α
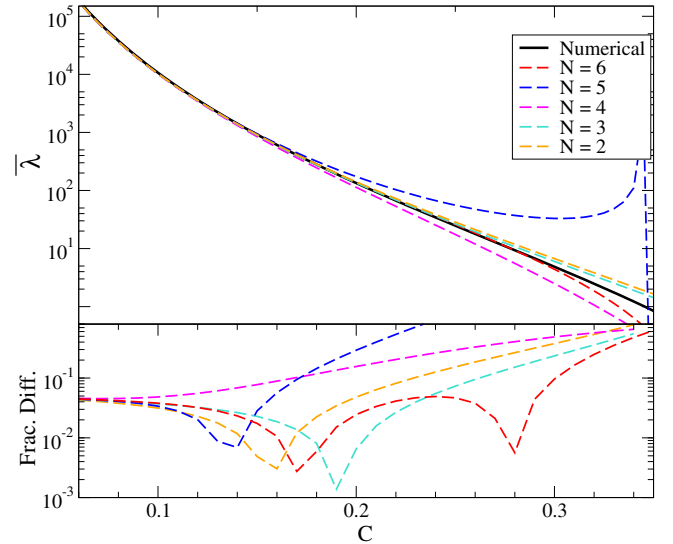

FIG. 5. Similar to Fig. 3 but for the Love-C relation. Observe that the series does not converge in this case and the third-order expansion gives the most accurate result.
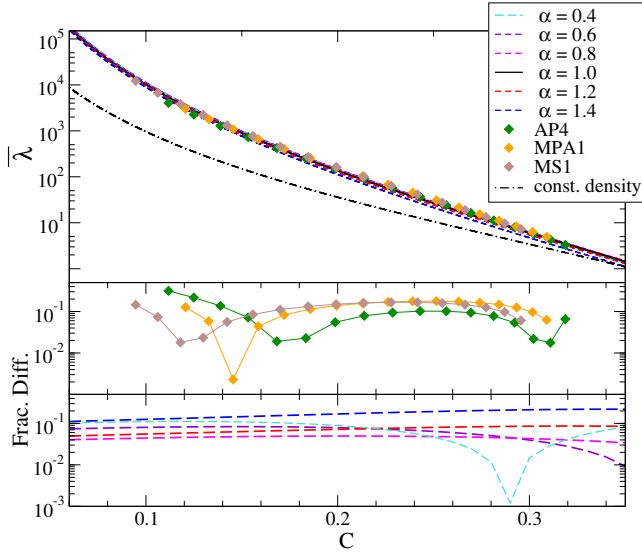
FIG. 6. Similar to Fig. 4 but for the Love-C relation. The analytic relations for the modified Tolman model have been kept up to third order in $\mathcal{C}$. Observe that the EOS variation is kept under $\mathcal{O}(10\%)$ for both modified Tolman VII and realistic EOSs, in agreement with that for realistic EOSs in Fig. 15 of Ref. [40].

is of the order of 10%, consistent with the EOS variation in the Love-C relation for realistic EOSs in the middle panel (see also [40]).

Similar to the I-C case, we can investigate further the amount of the α (or EOS) variation in the Love-C relation by expanding the analytic solution about the original Tolman solution. To achieve this, we first expand $\bar{\lambda}$ as

$$\bar{\lambda} \approx \sum_{n=0}^{N} \bar{\lambda}_n \mathcal{C}^n. \tag{47}$$

We then expand further each coefficient $\bar{\lambda}_n$ about $\alpha = 1$ and find

$$\bar{\lambda}_0 = 0.204[1 - 0.186(\alpha - 1) + \mathcal{O}(\alpha - 1)^2],$$
$$\bar{\lambda}_1 = -1.274[1 - 0.090(\alpha - 1) + \mathcal{O}(\alpha - 1)^2],$$
$$\bar{\lambda}_2 = 2.749[1 + 0.082(\alpha - 1) + \mathcal{O}(\alpha - 1)^2],$$
$$\bar{\lambda}_3 = -2.281[1 + 0.420(\alpha - 1) + \mathcal{O}(\alpha - 1)^2],$$
$$\bar{\lambda}_4 = 3.199[1 + 0.013(\alpha - 1) + \mathcal{O}(\alpha - 1)^2],$$
$$\bar{\lambda}_5 = -13.001[1 - 0.108(\alpha - 1) + \mathcal{O}(\alpha - 1)^2],$$
$$\bar{\lambda}_6 = 19.282[1 + 0.161(\alpha - 1) + \mathcal{O}(\alpha - 1)^2].$$

This expansion shows that the fractional α variation is only of the order of 10% or less for most of the coefficients, which again is consistent with the amount of EOS variation in the Love-C relation in Fig. 6. This gives us an analytic explanation for the amount of EOS variation in the relation.

V. I-LOVE RELATION

Now that we have calculated the moment of inertia and tidal deformability, we can construct semianalytic relations between these two quantities based on the modified Tolman VII solutions.

One can derive the I-Love relation ($\bar{I}$ as a function of $\bar{\lambda}$) semianalytically based on the analytic I-C and Love-C relations by parametrically plotting $\bar{I}$ and $\bar{\lambda}$. Namely, we choose one $\mathcal{C}$ and plot a point in the I-Love plane using the above two analytic relations. We then change $\mathcal{C}$ and repeat the procedure to find the I-Love relation. This is semianalytic in the sense that we are not providing a closed form expression of $\bar{I}$ in terms of $\bar{\lambda}$.

Regarding the Love-C relation, we found that the expansion to sixth order in $\mathcal{C}$ gives us a more accurate semianalytic I-Love relation than that with the third-order expansion, which is counterintuitive given that the sixth-order Love-C relation is less accurate than the third-order one. This behavior arises because the amount of inaccuracy in the sixth-order Love-C relation partially cancels with that in the I-C relation, producing a more accurate I-Love relation. For this reason, we will use the sixth-order Love-C relation for constructing the I-Love relation.

The top panel in Fig. 7 presents such semianalytic I-Love relations for the modified Tolman VII model. In most regimes, observe that the α variation shown in the bottom panel is of $\mathcal{O}(1\%)$ at most. This reproduces the amount of the EOS variation in the I-Love relations for realistic NSs shown in the middle panel and also found in Refs. [40,42,43]. The α variation becomes slightly larger when $\bar{I}$ and $\bar{\lambda}$ are smaller,
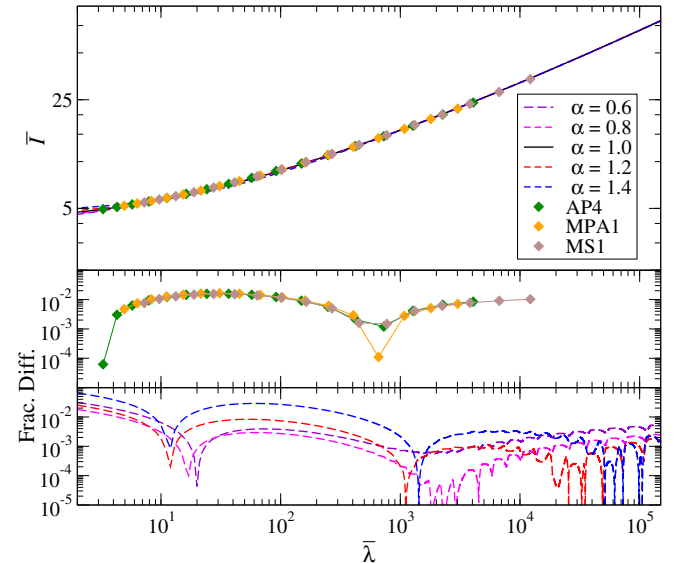

FIG. 7. (Top) Similar to Fig. 4 but for the I-Love relation. The semianalytic modified Tolman VII model is constructed by keeping the analytic I-C and Love-C relations up to sixth order in $\mathcal{C}$. Observe that the EOS variation is kept around 1% for both realistic EOSs and the modified Tolman VII model.

though this is due to the fact that the sixth-order Love-C relation becomes less accurate in the large $\mathcal{C}$ regime.

One can also obtain an approximate but completely analytic I-Love relation by first inverting the Love-C relation for $\mathcal{C}$ and substituting it to the I-C relation. For inverting the Love-C relation, one can find a series-expanded solution of the form

$$C = \sum_{n=0} \frac{a_n}{\bar{\lambda}^{n/5}}, \tag{48}$$

with the coefficient a_n that is a function of α. The analytic I-Love relation obtained in this way, however, is not very accurate, at least up to the (sixth) order that we have worked on. We found that the variation in α can be $\mathcal{O}(10\%)$ or larger, and one may need to increase the order of the expansion to find a more accurate relation, which we leave for future work.

One can improve the semianalytic model further by resumming the series-expanded I-C and Love-C (or the y_R expression to be more precise) relations using the Padé approximant. Such Padé expressions for the modified Tolman solutions are lengthy and not very useful, while we managed to derive a simple form for the original Tolman solution. The results are given in Eqs. (1)–(3), and the relations are shown in Fig. 1. For the Padé resummation, we found that the third-order expansion of $y(\mathcal{C})$ provides a more accurate, semianalytic I-Love relation (to be discussed in the next paragraph) than the sixth-order expansion. This is why the Padé resummation is of the order of (3,3) for the I-C relation while of the order of (2,2) for the Love-C relation.

The top panel in Fig. 8 presents the semianalytic I-Love relation for the original Tolman solution using the Padé expressions for the I-C and Love-C relations. For comparison, we also present the Padé-resummed relation for constant-density stars [48] and realistic NSs using all 11 EOSs considered in Fig. 2. The middle (bottom) panel shows the relative fractional difference between the relation with each EOS and the constant-density (Padé-resummed original Tolman) model. Observe that the original Tolman relation always agrees with the realistic models within an error of 1% and gives a more accurate description than the constant-density case especially in the large compactness (small $\bar{\lambda}$) regime. Comparing the bottom panel in Fig. 8 with the middle panel in Fig. 7, one sees that the former slightly has a smaller fractional error, and thus the Padé resummed I-Love relation indeed proves a more accurate result than the series-expanded one. We do not show the numerical fit for the I-Love curve found in Ref. [42], since it is indistinguishable from other curves and the fractional differences are around 1%.

VI. POSSIBLE ORIGIN OF THE UNIVERSALITY

We now try to connect our analytic calculations to possible origins of some of the universal relations.
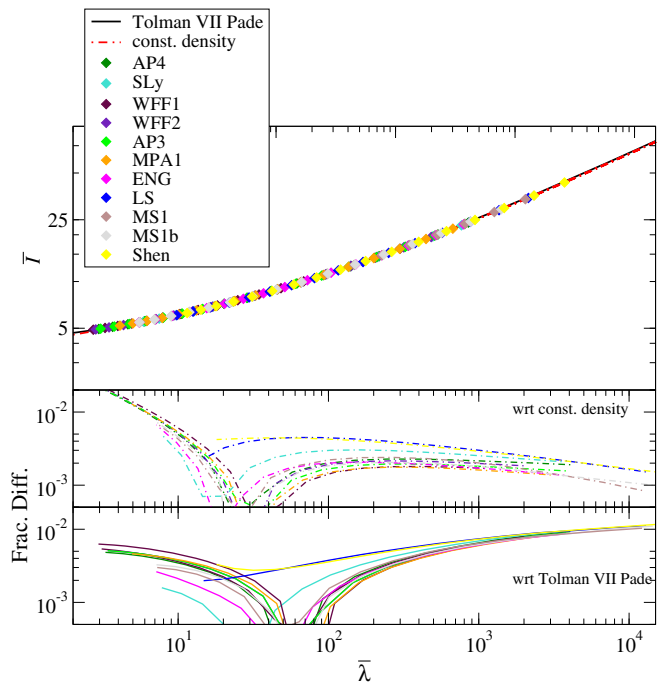

FIG. 8. (Top) Semianalytic, Padé-resummed I-Love relation for the original Tolman VII solution, together with the analytic relation for constant-density stars [48] and numerical results for realistic EOSs. (Middle) The relative fractional difference of the relations for the realistic EOSs from the analytic one for constant-density stars. (Bottom) Similar to the middle panel but for the Tolman VII relation. Observe that the Tolman VII model maintains universality with an EOS variation of less than 1% for the whole range of $\bar{\lambda}$.

Regarding the I-Love-Q relations, Ref. [46] showed that the universality is related to approximate self-similarity of isodensity contours inside NSs, and this self-similarity becomes exact for constant-density stars. Similarly, Ref. [47] demonstrated that the origin of the universality can be attributed to the fact that realistic EOSs for NSs are "similar" to constant-density EOSs, which is consistent with the findings in Ref. [46]. Unfortunately, these explanations do not apply to the I-C and Love-C relations, since NSs and constant-density stars do not share the universality.

Here, we aim to obtain some insight on the possible origin of the I-C and Love-C universal relations based on our analytic calculations presented in the previous sections. The original Tolman VII solution is a two-parameter model characterized by the stellar mass and radius and, thus, can explain any mass-radius relations for NSs. Yet, we found that there are unique I-C and Love-C relations for the Tolman VII solution that agree well with those found numerically with realistic EOSs. The underlying assumption in the Tolman VII solution is that the energy-density profile inside a star follows a quadratic function in the radial coordinate [Eq. (11)]. All of this suggests that one can attribute the origin of the I-C and
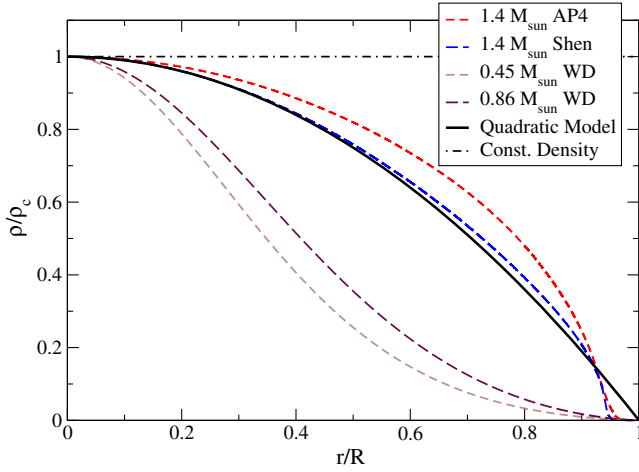
FIG. 9. The normalized energy-density profiles of NSs and white dwarfs, together with quadratic (original Tolman VII solution) and constant-density models. The fact that realistic NS profiles approximately follow the quadratic function in Eq. (11) (whereas constant-density stars and white dwarfs do not) can be interpreted as a possible origin of the I-C and Love-C universality.

Love-C universality to the fact that the energy-density profile for NSs roughly follows a quadratic function.

Figure 9 presents the energy-density profiles for realistic NSs, together with realistic white dwarfs, the Tolman VII quadratic model, and constant-density stars. Observe that the NS profiles can be approximated well with the quadratic model, while white dwarfs and constant-density stars have different profiles. Universal relations for white dwarfs have been studied, e.g., in Refs. [58–60], which showed that they were quite different from the NS ones. The modified Tolman VII model that we also considered in this paper accounts for the difference between the realistic NS profile and the quadratic one. As shown in the previous sections, we managed to recover the $\mathcal{O}(10\%)$ EOS variation analytically. Figure 9 together with these analytic calculations supports our claim that one possible origin of the universality for the I-C and Love-C relations is due to the fact that realistic NSs follow more or less the quadratic energy-density profile, and the deviation can explain the amount of the EOS variation in the relations.

VII. CONCLUSIONS AND DISCUSSIONS

In this paper, we derived analytic I-C and Love-C and semianalytic I-Love relations based on the modified

Tolman VII model. We used series expansion in compactness to solve differential equations and found approximate expressions for the moment of inertia and tidal deformability. Varying the modified Tolman VII parameter α that enters in the energy-density profile, we analytically showed the 10% EOS variation in the I-C and Love-C relations and the 1% EOS variation in the I-Love relation that are consistent with the amount found numerically [40]. Our analytic relations more accurately describe the relations for realistic NSs than the constant-density model [48] (more appropriate for quark stars [40]), especially for the I-C and Love-C relations. Our analytic relations are comparable to the fitted relations in their accuracy [40], and the former is based on a theoretical founding while the latter is phenomenological. Based on these analytic findings, we pointed out that a possible origin of the I-C and Love-C relations may be due to the energy-density profile for realistic NSs approximately following a quadratic function. This can explain why the constant-density stars deviate from the NS branch in these relations. Such an origin is different from that for the universality in the I-Love-Q relations discussed in Refs. [46,47].

Let us comment on a few possible directions for future work. One possibility includes improving the analytic results presented here. For example, one could try a different expansion in ξ or $\mathcal{C}$ for the Love-C relation, such as that in Ref. [61] for constant-density stars. One could then try to construct a more accurate inversion of the relation, so that an accurate, analytic I-Love relation can be derived. Another avenue includes deriving similar, analytic expressions for multipole moments, such as quadrupole and octupole, so that one could construct analytic, I-Love-Q relations [42,43] and "no-hair" relations [62–64] for neutron stars. One could also derive analytic expressions for multipolar tidal deformabilities and construct analytic multipole Love relations [65]. Such studies may further extend our knowledge of the origin of these universal relations.

[1] J. Lattimer and M. Prakash, Astrophys. J. **550,** 426 (2001).
[2] T. Guver and F. Ozel, Astrophys. J. **765,** L1 (2013).
[3] A. W. Steiner, J. M. Lattimer, and E. F. Brown, Astrophys. J. **722,** 33 (2010).
[4] J. M. Lattimer and A. W. Steiner, Eur. Phys. J. A **50,** 40 (2014).
[5] F. Ozel, D. Psaltis, T. Guver, G. Baym, C. Heinke, and S. Guillot, Astrophys. J. **820,** 28 (2016).
[6] F. Ozel and P. Freire, Annu. Rev. Astron. Astrophys. **54,** 401 (2016).
[7] A. W. Steiner, C. O. Heinke, S. Bogdanov, C. Li, W. C. G. Ho, A. Bahramian, and S. Han, Mon. Not. R. Astron. Soc. **476,** 421 (2018).
[8] T. E. Riley, A. L. Watts, S. Bogdanov, P. S. Ray, R. M. Ludlam, S. Guillot, Z. Arzoumanian, C. L. Baker, A. V. Bilous, D. Chakrabarty, K. C. Gendreau, A. K. Harding, W. C. G. Ho, J. M. Lattimer, S. M. Morsink, and T. E. Strohmayer, Astrophys. J. **887,** L21 (2019).
[9] M. C. Miller *et al.*, Astrophys. J. **887,** L24 (2019).
[10] S. Bogdanov *et al.*, Astrophys. J. **887,** L25 (2019).
[11] S. Bogdanov, F. K. Lamb, S. Mahmoodifar, M. C. Miller, S. M. Morsink, T. E. Riley, T. E. Strohmayer, A. K. Tung, A. L. Watts, A. J. Dittmann, D. Chakrabarty, S. Guillot, Z. Arzoumanian, and K. C. Gendreau, Astrophys. J. **887,** L26 (2019).
[12] S. Guillot *et al.*, Astrophys. J. **887,** L27 (2019).
[13] G. Raaijmakers, T. E. Riley, A. L. Watts, S. K. Greif, S. M. Morsink, K. Hebeler, A. Schwenk, T. Hinderer, S. Nissanke, S. Guillot, Z. Arzoumanian, S. Bogdanov, D. Chakrabarty, K. C. Gendreau, W. C. G. Ho, J. M. Lattimer, R. M. Ludlam, and M. T. Wolff, Astrophys. J. **887,** L22 (2019).
[14] J.-E. Christian and J. Schaffner-Bielich, Astrophys. J. Lett. **894,** L8 (2020).
[15] J.-L. Jiang, S.-P. Tang, Y.-Z. Wang, Y.-Z. Fan, and D.-M. Wei, Astrophys. J. **892,** 1 (2020).
[16] G. Raaijmakers *et al.*, Astrophys. J. Lett. **893,** L21 (2020).
[17] J. Zimmerman, Z. Carson, K. Schumacher, A. W. Steiner, and K. Yagi, arXiv:2002.03210.
[18] T. Dietrich, M. W. Coughlin, P. T. H. Pang, M. Bulla, J. Heinzel, L. Issa, I. Tews, and S. Antier, arXiv:2002.11355.
[19] P. B. Demorest, T. Pennucci, S. M. Ransom, M. S. E. Roberts, and J. W. T. Hessels, Nature (London) **467,** 1081 (2010).
[20] J. Antoniadis, P. C. Freire, N. Wex, T. M. Tauris, R. S. Lynch *et al.*, Science **340,** 1233232 (2013).
[21] H. T. Cromartie *et al.*, Nat. Astron. **4,** 72 (2020).
[22] M. Kramer and N. Wex, Classical Quantum Gravity **26,** 073001 (2009).
[23] J. M. Lattimer and B. F. Schutz, Astrophys. J. **629,** 979 (2005).
[24] T. Hinderer, Astrophys. J. **677,** 1216 (2008).
[25] E. E. Flanagan and T. Hinderer, Phys. Rev. D **77,** 021502 (2008).
[26] B. Abbott, R. Abbott, T. Abbott, F. Acernese, K. Ackley, C. Adams, T. Adams, P. Addesso, R. Adhikari, V. Adya *et al.*, Phys. Rev. Lett. **121,** 161101 (2018).
[27] B. P. Abbott *et al.* (LIGO Scientific, Virgo Collaborations), Phys. Rev. Lett. **121,** 161101 (2018).
[28] E. Annala, T. Gorda, A. Kurkela, and A. Vuorinen, Phys. Rev. Lett. **120,** 172703 (2018).
[29] B. P. Abbott *et al.* (LIGO Scientific, Virgo Collaborations), Phys. Rev. Lett. **121,** 161101 (2018).
[30] C. Raithel, F. Ozel, and D. Psaltis, Astrophys. J. **857,** L23 (2018).
[31] Y. Lim and J. W. Holt, Phys. Rev. Lett. **121,** 062701 (2018).
[32] A. Bauswein, O. Just, H.-T. Janka, and N. Stergioulas, Astrophys. J. **850,** L34 (2017).
[33] S. De, D. Finstad, J. M. Lattimer, D. A. Brown, E. Berger, and C. M. Biwer, Phys. Rev. Lett. **121,** 091102 (2018); **121,** 259902(E) (2018).
[34] E. R. Most, L. R. Weih, L. Rezzolla, and J. Schaffner-Bielich, Phys. Rev. Lett. **120,** 261103 (2018).
[35] E. Annala, T. Gorda, A. Kurkela, J. Nättilä, and A. Vuorinen, arXiv:1903.09121.
[36] T. Malik, N. Alam, M. Fortin, C. Providência, B. K. Agrawal, T. K. Jha, B. Kumar, and S. K. Patra, Phys. Rev. C **98,** 035804 (2018).
[37] Z. Carson, A. W. Steiner, and K. Yagi, Phys. Rev. D **99,** 043010 (2019).
[38] Z. Carson, A. W. Steiner, and K. Yagi, Phys. Rev. D **100,** 023012 (2019).
[39] C. A. Raithel and F. Ozel, Astrophys. J. **885,** 121 (2019).
[40] K. Yagi and N. Yunes, Phys. Rep. **681,** 1 (2017).
[41] D. D. Doneva and G. Pappas, Astrophysics and Space Science Library **457,** 737 (2018).
[42] K. Yagi and N. Yunes, Science **341,** 365 (2013).
[43] K. Yagi and N. Yunes, Phys. Rev. D **88,** 023009 (2013).
[44] K. Yagi and N. Yunes, Classical Quantum Gravity **33,** 13LT01 (2016).
[45] K. Yagi and N. Yunes, Classical Quantum Gravity **34,** 015006 (2017).
[46] K. Yagi, L. C. Stein, G. Pappas, N. Yunes, and T. A. Apostolatos, Phys. Rev. D **90,** 063010 (2014).
[47] Y.-H. Sham, T. K. Chan, L.-M. Lin, and P. T. Leung, Astrophys. J. **798,** 121 (2015).
[48] T. K. Chan, A. P. O. Chan, and P. T. Leung, Phys. Rev. D **91,** 044017 (2015).
[49] R. C. Tolman, Phys. Rev. **55,** 364 (1939).
[50] N. Jiang and K. Yagi, Phys. Rev. D **99,** 124029 (2019).
[51] https://github.com/nj2nu/I-C_Love-C_6thorderSeries Expansion_Coefficients.
[52] A. Maselli, V. Cardoso, V. Ferrari, L. Gualtieri, and P. Pani, Phys. Rev. D **88,** 023007 (2013).
[53] M. Urbanec, J. C. Miller, and Z. Stuchlik, Mon. Not. R. Astron. Soc. **433,** 1903 (2013).
[54] J. B. Hartle, Astrophys. J. **150,** 1005 (1967).
[55] C. Breu and L. Rezzolla, Mon. Not. R. Astron. Soc. **459,** 646 (2016).
[56] K. V. Staykov, D. D. Doneva, and S. S. Yazadjiev, Phys. Rev. D **93,** 084010 (2016).
[57] T. Damour and A. Nagar, Phys. Rev. D **80,** 084035 (2009).
[58] K. Boshkayev, H. Quevedo, and B. Zhami, Mon. Not. R. Astron. Soc. **464,** 4349 (2017).
[59] K. Boshkayev and H. Quevedo, Mon. Not. R. Astron. Soc. **478,** 1893 (2018).
[60] A. Taylor, K. Yagi, and P. Arras, Mon. Not. R. Astron. Soc. **492,** 978 (2020).
[61] D. Petroff, Classical Quantum Gravity **24,** 1055 (2007).

[62] L. C. Stein, K. Yagi, and N. Yunes, Astrophys. J. **788**, 15 (2014).

[63] K. Yagi, K. Kyutoku, G. Pappas, N. Yunes, and T. A. Apostolatos, Phys. Rev. D **89**, 124013 (2014).

[64] B. Majumder, K. Yagi, and N. Yunes, Phys. Rev. D **92**, 024020 (2015).

[65] K. Yagi, Phys. Rev. D **89**, 043011 (2014); **96**, 129904(E) (2017); **97**, 129901(E) (2018).